Chinese Chemical Letters 36 (2025) 109913

Contents lists available at ScienceDirect

Chinese Chemical Letters

journal homepage: www.elsevier.com/locate/cclet

Covalent modulation of mPGES1 activity *via* α,β-unsaturated aldehyde group: Implications for downregulating PGE2 expression and antipyretic response

Fuyun Chi, Man Zhang, Yiman Han, Fukui Shen, Shijie Peng, Bo Su, Yuanyuan Hou*, Gang Bai*

State Key Laboratory of Medicinal Chemical Biology, College of Pharmacy and Tianjin Key Laboratory of Molecular Drug Research, Nankai University, Tianjin 300353, China

ARTICLE INFO

Article history:
Received 24 February 2024
Revised 17 April 2024
Accepted 19 April 2024
Available online 20 April 2024

Keywords:
α,β-Unsaturated aldehyde
Covalent binding
mPGES1
PGE2
Antipyretic

ABSTRACT

Prostaglandin E2 (PGE2) serves as the ultimate mediator of fever induced by inflammatory factors. In contrast to cyclooxygenase inhibitors that suppress arachidonic acid metabolism, antipyretic herbs possess a well-established clinical history in effectively managing fever. However, the specific mechanisms underlying their efficacy remain unclear. Following the screening for lead compounds that inhibit PGE2 from antipyretic herbs, alkynylated active molecule probes were designed and synthesized to track and identify potential targets. The target investigation revealed that three antipyretic compounds, namely cinnamaldehyde, 2,4-decadienal, and perillaldehyde, containing α,β-unsaturated aldehyde groups irreversibly targeted the microsomal PGES1-TM4 helix (mPGES1-TM4) at Ser139. This specific interaction effectually inhibited PGE2 production in the cerebral vasculature, leading to exert potent antipyretic effects. α,β-Unsaturated aldehydes targeting mPGES1-TM4 offer a new approach for antipyretic effects with significant potential for various applications.

Covalent drugs block protein function by forming a specific bond between the ligand and the target protein. A covalent mechanism of action provides many pharmacological advantages over a reversible mechanism of action, including enhanced potency, selectivity and prolonged duration of action [1]. Natural products represent an indispensable reservoir for the development of covalent drugs, most of which target proteins [2]. Cysteine, lysine, serine, *etc.*, possess nucleophilic functional groups such as sulfhydryl, amino, hydroxyl, capable of reacting with drugs with electrophilic warheads like epoxide, halogen, carbonyl, isocyanine and other groups to form covalent bonds [3]. In the case of electrophilic natural products, the covalent nature of their target interaction has largely facilitated the identification of their biological targets. The discovery of the epoxide-containing natural product, trapoxin, established a class of histone deacetylases as new drug targets against cancer [4]. The pancreatic lipase inhibitor lipstatin, whose structure features a β-lactone ring, undergoes nucleophilic attack by a serine residue that blocks of the active site of the lipase, inhibiting protein function and fat turnover [5]. Endogenous electrophiles, such as α,β-unsaturated aldehydes generated during lipid peroxidation, exhibit a facile reactivity with proteins, generating a variety of intra- and inter- molecular covalent adducts. These host-derived modified proteins with electrophiles constitute the products of diverse classes of oxidative reactions and represent damage-associated molecular patterns (DAMPs) [6,7].

Prostaglandin E2 (PGE2) is the ultimate mediator of fever induced by inflammatory factors, a product of arachidonic acid and other polyunsaturated fatty acid metabolism catalyzed by cell membrane phospholipids. As the most abundant prostaglandin in the human body, PGE2 plays an indispensable role in the pathogenesis of inflammation and fever [8]. During PGE2 metabolism and synthesis, free arachidonic acid (AA) is enzymatically converted by COX1/2 into prostaglandin G2 (PGG2), which is subsequently reduced into the precursor metabolite, prostaglandin H2 (PGH2) [9]. Prostaglandin E2 synthases (PGESs), also known as terminal synthases, catalyze the biosynthesis of active PGE2 from PGH2 derived from COX1 and COX2 enzymes, representing the final step in PGE2 biosynthesis. To date, three types of PGESs have been identified: microsomal PGES1 (mPGES1), microsomal PGES2 (mPGES2), and cytosolic PGES (cPGES) [10]. In contrast to the constitutively expressed cPGES and mPGES2, mPGES1 is an inducible

* Corresponding authors.
E-mail addresses: houyy@nankai.edu.cn (Y. Hou), gangbai@nankai.edu.cn (G. Bai).

https://doi.org/10.1016/j.cclet.2024.109913
1001-8417/

enzyme that specifically couples with COX2 [11,12]. The expression of mPGES1 is induced by inflammatory stimuli, including interleukin-1-beta (IL-1β) [13]. The induction of mPGES1 by inflammatory stimuli and its role in the production of COX2-derived PGE2 make it a viable alternative target of COX2 for managing inflammatory conditions [14].

In this study, we screened traditional heat-clearing herbs to identify their active ingredients based on their antipyretic effect and the generation of PGE2. Subsequently, representative monomeric probes were synthesized, and a series of chemical biology techniques were employed for target tracing and identification [15,16]. Through the verification experiment of AA-PGE2 oxidized lipidomics and protein profile identification, it has been demonstrated that certain specific volatile components containing an α,β-unsaturated aldehyde group possess the potential to irreversibly bind mPGES1 and exert antipyretic effects. The animal experiments were approved by the Animal Ethics Committee, Nankai university (Tianjin, China) and were performed in accordance with the guidelines of the national legislation of China. The use and care of animal for the study described herein was approved (No. 2022-SYDWLL-000491). The material information and detailed experimental procedures are described in Supporting information.

Given that PGE2 serves as the principal mediator of fever, the inhibitory effects of 24 extracts derived from antipyretic herbs on the expression of PGE2 were investigated in RAW 264.7 cells. The significant inhibitory effects of *Cinnamomi ramulus* (CR), *Perillae folium* (PF), *Zingiber officinale* Roscoe (ZRR), and *Radix Bupleuri* (BR) on PGE2 production were demonstrated (Fig. S1 in Supporting information). To further investigate their efficacy, the different polar layers of the aforementioned extracts were evaluated for their impact on PGE2 expression. The components of the volatile oil, primarily presented in the dichloromethane (DCM) or ethyl acetate (EA) extraction layer, significantly attenuated the lipopolysaccharide (LPS)-induced upregulation of PGE2 expression (Fig. S2 in Supporting information). Furthermore, the four primary constituents, namely cinnamaldehyde (CA), perillaldehyde (PA), 6-shogaol (SOL), and 2,4-decadienal (DAL), were derived from the corresponding volatile oils of these herbal sources and effectively alleviated LPS-induced hyperthermia *in vivo*, as evidenced by thermographic imaging (Fig. 1A). However, the corresponding components lacking α,β-unsaturated group named PPA, PAR, POL and DL did not affect PGE2 expression (Figs. 1B and C). The results suggested that the α,β-unsaturated group may play a crucial role in combating LPS-induced fever.

As a primary constituent of cinnamon volatile oil, CA was chosen for further investigation due to its superior antipyretic effect. The comparative analysis involved cinnamic acid (CAC), cinnamyl alcohol (CALC), and benzylacetone (BA) as controls, wherein the α,β-unsaturated aldehyde group was modified to carboxyl, hydroxyl and ketone groups (Fig. 2A). The results in Fig. 2B demonstrated that only CA and CA probes derived with the alkynyl group possess the ability to suppress PGE2 expression, indicating that α,β-unsaturated aldehyde group plays a pivotal role in exerting its antipyretic activity. Then, the CA probe was applied to capture potential targets in RAW 264.7 cells. The target fhing efficiency was assessed by sodium dodecyl sulphate-polyacrylamide gel electrophoresis (SDS-PAGE) analysis (Fig. 2C), and the enriched bands were subjected to enzymatic digestion followed by identification through high performance liquid chromatography-mass spectrometry/mass spectrometry (HPLC-MS/MS) analysis. All proteins associated with the antipyretic process from the human gene database (https://www.genecards.org/) were utilized for comprehensive analysis, along with the captured and identified proteins. As shown in Fig. 2D, four potential targets (mPGES1, ANXA5, C1qBP, and TRIM28) were proposed, of which only mPGES1 was associated with the AA-PGE2 pathway. Subsequently, mPGES1 was

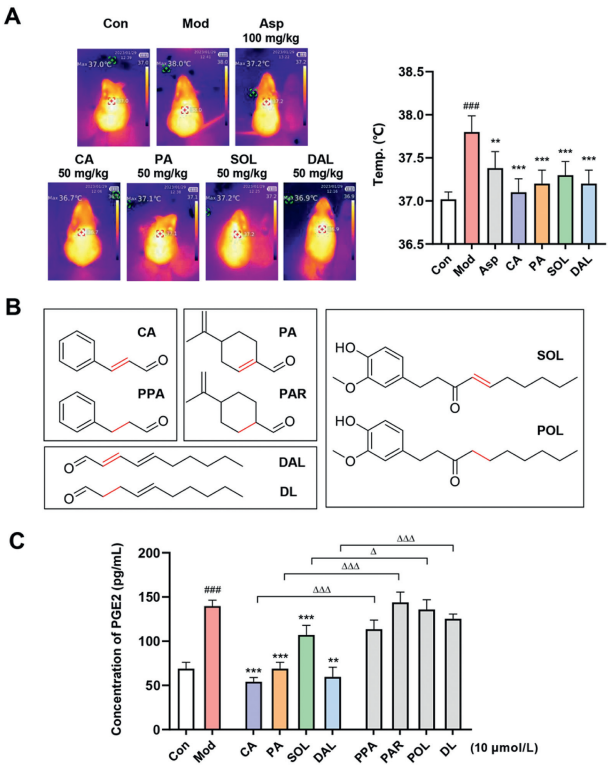

Fig. 1. Monomeric compounds containing α,β-unsaturated group inhibit PGE2 production. (A) Antipyretic effects of CA, PA, SOL and DAL against LPS-induced fever in mice ($n=5$). (B) Chemical structures of CA, PA, SOL, and DAL along with α,β-unsaturated double bond disrupted compounds. (C) The inhibition effects of CA, PA, SOL and DAL and its corresponding derivates on PGE2 expression in RAW 264.7 cells ($n=3$). $^{\#\#\#}P<0.001$ *vs.* Con group; $^{***}P<0.001$, $^{**}P<0.01$ *vs.* Mod group; $^{\triangle\triangle\triangle}P<0.001$, $^{\triangle}P<0.05$ *vs.* prototype compound. Data are presented as mean ± standard deviation (SD).

hypothesized to be a potential target and confirmed by Western blot (Fig. 2E). As expected, the CA probe capturing demonstrated no interaction with PTGS2 and COX2, which are crucial enzymes in the AA-PGE2 pathway.

After incubating RAW 264.7 cells with a 10 μmol/L CA probe, the in-gel imaging assay revealed the position of mPGES1 was specific metabolic labeled (Fig. 2F). However, no specific results were observed following treatment with 10 μmol/L CA. Additionally, a co-localization test was conducted between mPGES1 and the CA, which demonstrated that CA probe strongly merged with mPGES1 in RAW 264.7 cells (Fig. 2G). While knockout of mPGES1 resulted in a weakened merged yellow observed in cells with silenced mPGES1 (Figs. S3 and S4 in Supporting information). These findings suggest that mPGES1 is one of the target proteins of CA in antipyretic.

To confirm the significance of α,β-unsaturated aldehyde as a crucial pharmacophore in inhibiting PGE2 activity, another antipyretic compound, DAL, was chosen to validate its structure-activity relationship. To clarify the primary target of DAL, a α,β-unsaturated double bond-reduced analogue (DL) and a DAL probe were designed and employed. The structures are depicted in Fig. 3A. Reaffirming our expectations, both DAL and the DAL probe demonstrated bio-equivalence by inhibiting LPS-induced PGE2 expression, whereas DL did not exhibit such inhibition (Fig. 3B). Similarly, the proteins captured by the DAL probe in the AA-PGE2 pathway were verified using SDS-PAGE and Western blot, which demonstrated that mPGES1 could potentially be targeted by DAL (Figs. 3C and D). After preincubation with 10 μmol/L DAL probe, an in-gel imaging assay revealed that the DAL probe clearly

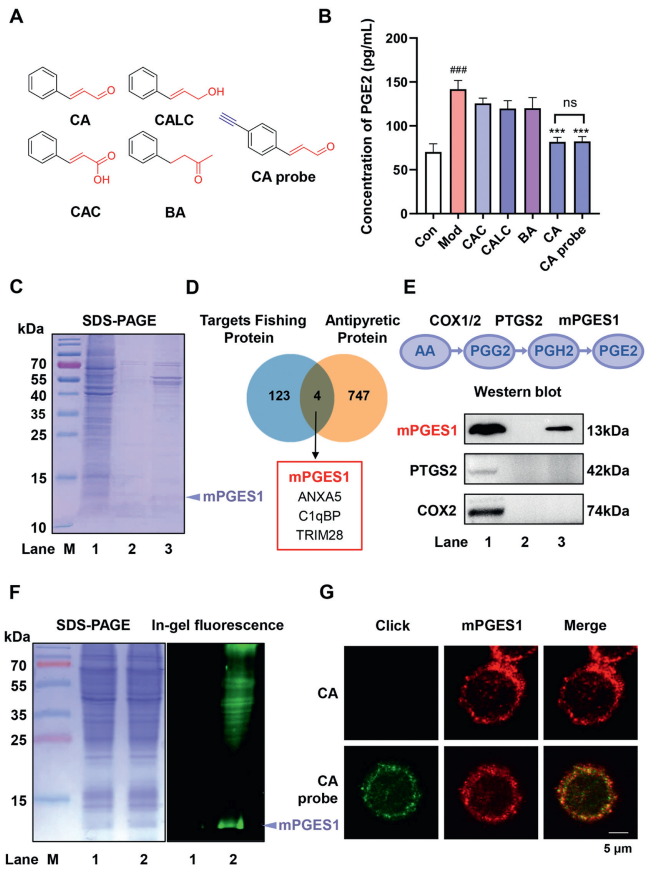

Fig. 2. mPGES1 is identified as a potential target of CA. (A) Structure of CA, CAC, CALC, BA and CA probe. (B) The inhibition effects of CA, CAC, CALC, BA and CA probe (10 μmol/L) on PGE2 expression in RAW 264.7 cells ($n = 3$). $^{###}P < 0.001$ *vs.* Con group; $^{***}P < 0.001$ *vs.* Mod group. Data are presented as mean ± SD. (C) The capture efficiency evaluation of CA probe using SDS-PAGE followed by Coomassie brilliant blue staining. Lane 1: RAW 264.7 cell total lysate; Lane 2: a negative control performed by blank magnetic microspheres (MMs); Lane 3: magnetic captured proteins by CA probe modified MMs. (D) Venn diagram analysis of CA probe enriched protein and antipyretic related targets. (E) Western blot analysis of captured protein by CA probe in RAW 264.7 cells. Lane 1: RAW 264.7 cell total lysate, Lane 2: a negative control performed by blank MMs; Lane 3: magnetic captured proteins by CA probe modified MMs. (F) In-gel imaging for CA (10 μmol/L) or CA probe (10 μmol/L) incubated RAW 264.7 cells. Lane 1: CA; Lane 2: CA probe. (G) The co-localization assay between mPGES1 and CA probe (10 μmol/L) on RAW 264.7 cells.

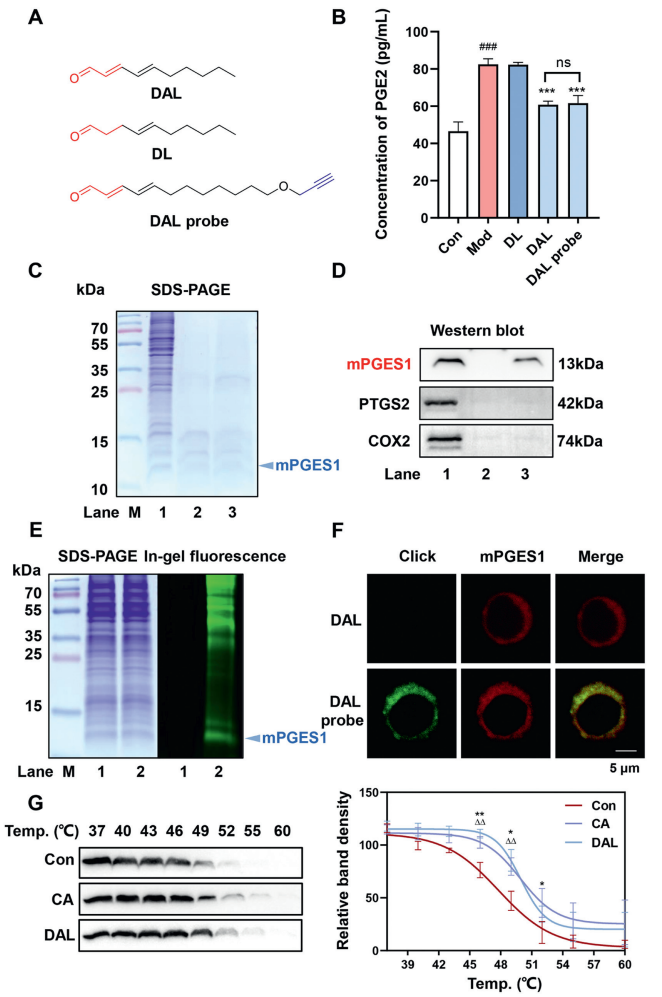

Fig. 3. α,β-Unsaturated aldehyde is suggested as the key pharmacophore. (A) Structure of DAL, DL, and DAL probe. (B) The inhibition effects of DAL, DL, DAL probe (10 μmol/L) on PGE2 expression in RAW 264.7 cells ($n = 3$). $^{###}P < 0.001$ *vs.* Con group; $^{***}P < 0.001$ *vs.* Mod group. (C, D) SDS-PAGE and Western blot analysis for captured protein by DAL probe. Lane 1: RAW 264.7 cell total lysate; Lane 2: a negative control performed by blank MMs; Lane 3: DAL probe magnetic captured proteins. (E) In-gel imaging for DAL (10 μmol/L) or DAL probe (10 μmol/L) incubated RAW 264.7 cells. Lane 1: DAL; Lane 2: DAL probe. (F) The co-localization assay between mPGES1 and DAL probe on RAW 264.7 cells. (G) CETSA for mPGES1 with CA (10 μmol/L) or DAL (10 μmol/L) tretmeant, which evaluated by Western blot ($n = 3$). $^{**}P < 0.01$, $^{*}P < 0.05$ represent CA group *vs.* Con group. $^{\triangle\triangle}P < 0.01$, $^{\triangle}P < 0.05$ represent DAL group *vs.* Con group. Data are presented as mean ± SD.

formed covalent bonds with mPGES1 (Fig. 3E). Furthermore, a co-localization test also indicated the successful co-localization of the DAL probe with mPGES1 in the cytoplasm of RAW 264.7 cells (Fig. 3F).

Finally, the interaction between CA or DAL and mPGES1 was performed using cellular thermal shift assay (CETSA). As shown in Fig. 3G, the covalent binding of CA or DAL to mPGES1 significantly enhanced its thermal stability. These findings collectively revealed that the α,β-unsaturated aldehyde group plays a crucial role in specifically targeting mPGES1 for antipyretic effects.

The subunits of mPGES1 form a homotrimeric structure consisting of three transmembrane helices (TM1: Pro11–Lys41, TM2: Ser61–Ser90, and TM3: Pro96–Gly119), with additional TM4 helix-spanning residues (Pro124–His151) to complete the four-transmembrane helix architecture (Fig. 4A) [10]. To provide additional insights into the interaction of CA or DAL and mPGES1, molecular docking with potential covalent binding poses was performed for CA or DAL with mPGES1 (PDB: 4AL0). Notably, the top-scoring poses were visualized as 3D maps, revealing that both the α,β-unsaturated aldehyde group of CA or DAL form a irreversible binding with the hydroxy group of Ser139 in TM4 (Fig. 4B).

To verify the prediction of molecular docking, CA or DAL was incubated with the TM4 helix-spanning residues of the mPGES1 protein and the binding products were identified using protein profiling. As shown in Fig. 4C, for the b^+ and y^+ ion fragments of TM4 incubated with CA, the mass shift *m/z* between the $b_{15}{}^{2+}$-H_2O and $b_{16}{}^{2+}$ ion fragments was 118.56 Da. Since the b^+ ion carried two charges (b^{2+}), the mass shift (237.12 Da) between $b_{15}{}^{+}$-H_2O and $b_{16}{}^{+}$ was consistent with the mass of Ser+CA. It indicated that the corresponding amino acid sequence of Ser139 in mPGES1was labeled with CA (219.15 Da). Similarly, the mass shift *m/z* between the $y_{12}{}^{2+}$ and $y_{13}{}^{2+}$ ion fragments was 109.56 Da, and since y^+ ion fragments carried two charges (y^{2+}). The mass shift between $y_{12}{}^{+}$ and $y_{13}{}^{+}$ (219.11 Da) was consistent with the mass of Ser+CA-H_2O, suggesting that the Ser139 of mPGES1 was labeled with CA. The similar results were obtained for profiling TM4 incubated with DAL, showing a consistent pattern as depicted in Fig. 4D. The observed mass shift *m/z* corresponded to the mass of the respective

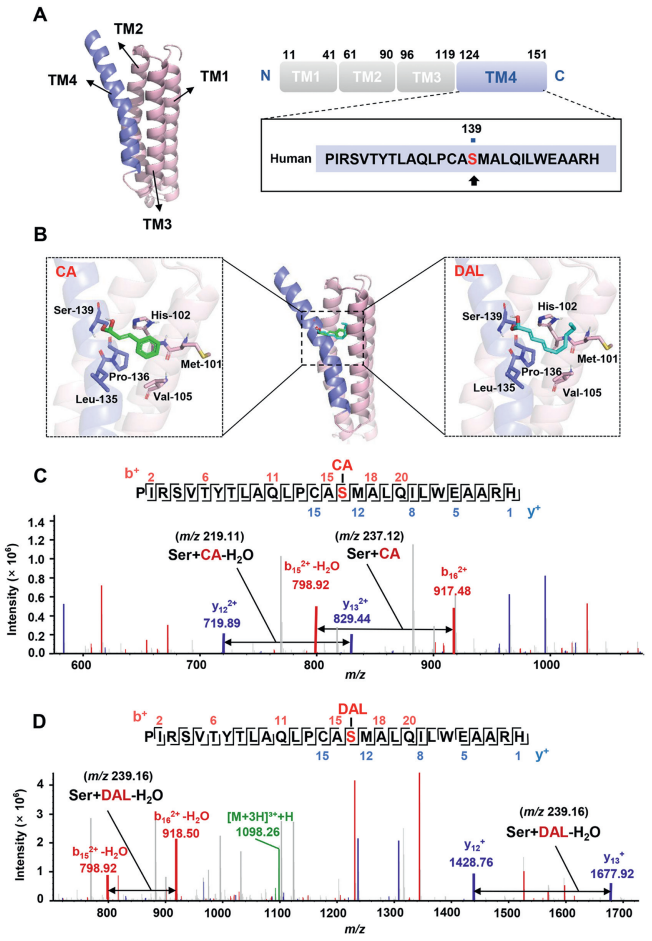

Fig. 4. CA and DAL covalent bind with mPGES1-TM4 at Ser139. (A) The schematic 3D structure and the sequence of mPGES1. (B) Molecular docking of CA and DAL with mPGES1. The b^+ and y^+ fragment ions of mPGES1-TM4 were detected by MS/MS after pretreatment with 100 μmol/L CA (C) or 100 μmol/L DAL (D).

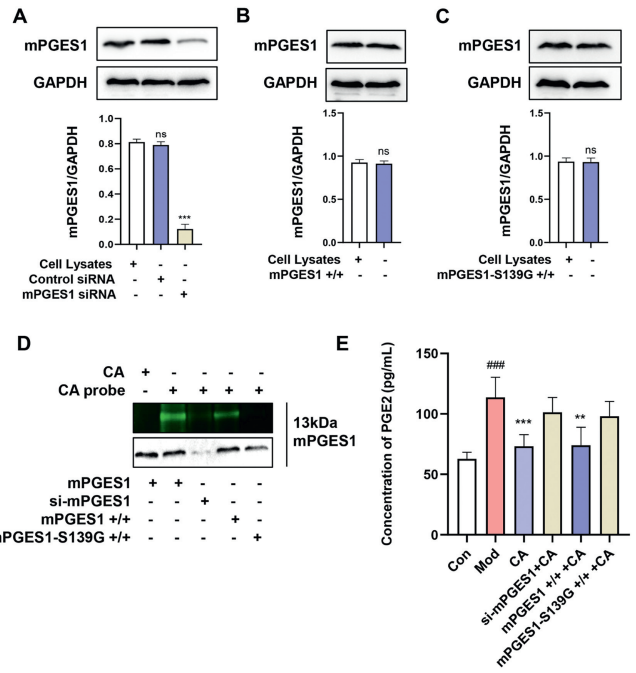

Fig. 5. CA specifically binds to Ser139 of mPGES1 to inhibit PGE2 production. (A–C) Western blot analysis for mPGES1 knockout and mPGES1 wild type or mPGES1-S139G mutant reconstruction in HEK 293T cells. In-gel imaging (D) and inhibition test of PGE2 (E) were conducted during the knockout and reconstruction of mPGES1 and mPGES1-S139G. $^{\#\#\#}P < 0.001$ *vs.* Con group; $^{**}P < 0.01$, $^{***}P < 0.001$ *vs.* Mod group ($n = 3$). GAPDH, glyceraldehyde-3-phosphate dehydrogenase. Data are presented as mean ± SD.

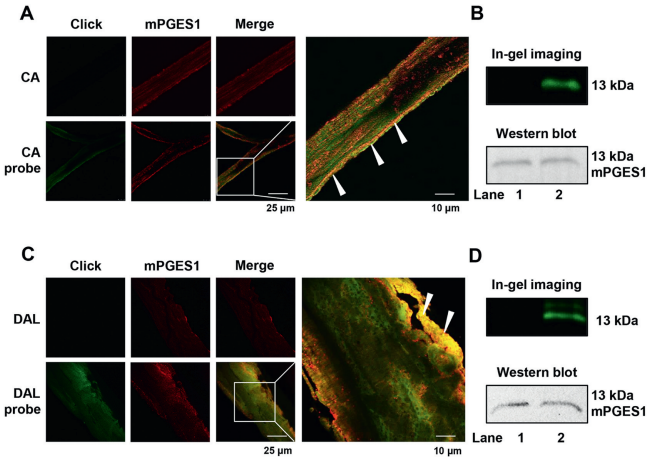

Fig. 6. CA and DAL bind to mPGES1 in the cerebral vasculature. (A) The co-localization assay between mPGES1 and CA probe (10 μmol/L) in rat cerebral vasculature. (B) In-gel imaging and Western blot assay for CA (10 μmol/L) or CA probe (10 μmol/L) pre-incubated rat cerebral vasculature. Lane 1: CA; Lane 2: CA probe. (C) The co-localization assay between mPGES1 and DAL probe (10 μmol/L) in rat cerebral vasculature. (D) In-gel imaging and Western blot assay for DAL (10 μmol/L) or DAL probe (10 μmol/L) pre-incubated rat cerebral vasculature. Lane 1: DAL; Lane 2: DAL probe.

TM4 fragment labeled with DAL (239.21 Da). These findings suggest that Ser139 in mPGES1 was also labeled with DAL.

Additionally, we characterized the irreversible bonding between mPGES1-TM4 and the other antipyretic molecues, PA and SOL (Figs. S5 and S6 in Supporting information). Due to the aldehyde group exhibits higher reactivity compared to the ketone group, the results demonstrated that PA could form a covalent bond with Ser139 in the mPGES1-TM4 fragment, whereas SOL, which contains α,β-unsaturated ketone group, did not exhibit the binding affinity. In summary, it was elucidated that only the α,β-unsaturated aldehyde group had the ability to covalently bind to Ser139 in the mPGES1-TM4.

To prove the above hypothesis, knockdown/reconstruction of mPGES1 was performed in HEK 293T cells (Figs. 5A–C). Upon reconstitution of wild type mPGES1 expression, an in-gel imaging assay revealed a clear metabolic labeling with the CA probe. However, no specific results were observed upon reconstitution of mPGES1-S139G mutant cells (Fig. 5D). The consistent findings were also corroborated by silencing mPGES1 in RAW 264.7 cells during the co-localization assay (Figs. S3 and S4 in Supporting information). Furthermore, the observation was consistent with the impact of CA on PGE2 production by the mPGES1 inhibition test (Fig. 5E). These findings strongly indicated that residue Ser139 is the exclusive binding site for CA on mPGES1.

A previous study demonstrated that knockdown of COX2 or mPGES1 specifically in the brain endothelial vasculature significantly ameliorated LPS-induced fever in mice, whereas silencing COX2 in neuronal or myeloid cells did not exert a significant impact on mouse body temperature [17]. These findings suggest that PGE2, synthesized in cerebral vascular endothelial cells, plays a critical role in mediating the fever response within the body.

To accurately determine the localization of CA in brain endothelial vessels, CA probe was pre-incubated with detached rat brain vessels, allowing for the visualization of co-localization between mPGES1 and the CA probe (Fig. 6A). In-gel imaging and

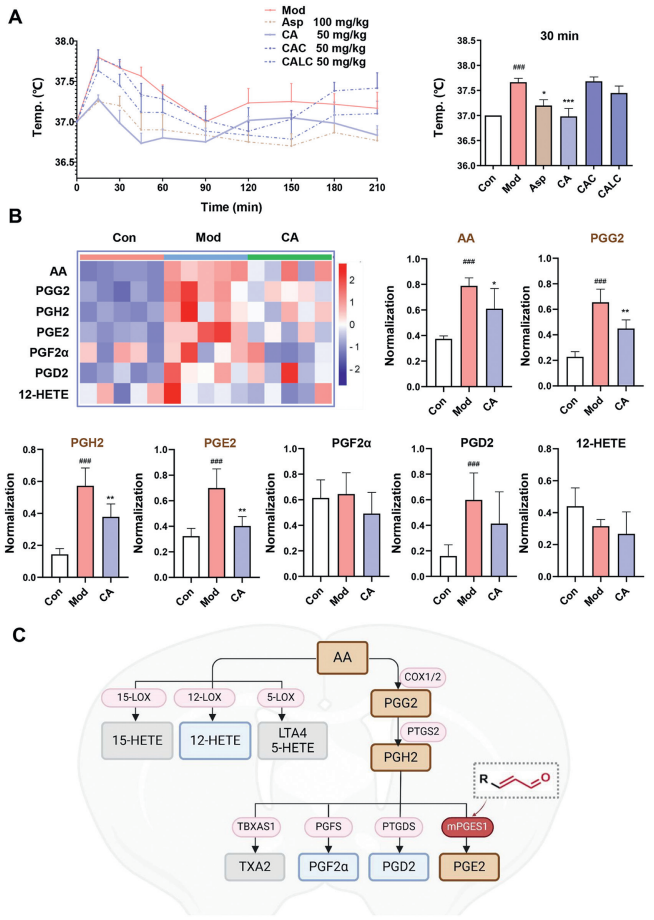

Fig. 7. CA inhibits the expression of key metabolites in the AA-PGE2 pathway and exerts antipyretic effects. (A) Inhibition effects of CA, CAC and CALC on LPS-induced anal temperature in rats ($n = 5$). (B) Quantitative metabolomics analysis of CA on the expression of oxidized lipids in rat brain tissue ($n = 5$). (C) Schematic diagram of α,β-unsaturated aldehyde group in affecting key metabolites on AA-PGE2 pathway. $^{###}P < 0.001$ *vs.* Con group; $^{***}P < 0.001$, $^{**}P < 0.01$, $^{*}P < 0.05$ *vs.* Mod group. Data are presented as mean ± SD.

Western blot further revealed that mPGES1 formed covalent bonds with the CA probe in the cerebral vasculature compared to unlabeled CA (Fig. 6B). Similar results were obtained for the DAL probe pre-incubation groups (Figs. 6C and D). The findings suggested that the α,β-unsaturated aldehyde compound exhibits irreversible binding to brain endothelial vasculature through its interaction with mPGES1.

To investigate the *in vivo* antipyretic mechanism of compounds containing the α,β-unsaturated aldehyde group, a febrile model was established in Sprague-Dawley rats induced by LPS. CA was selected as a representative drug, while CAC and CALC were included as control groups. The antipyretic effects on body temperature were assessed using anal temperature measurements (Fig. 7A). Notably, CA significantly attenuated the changes in body temperature, particularly at the 30-min time point, compared to the Mod group. However, neither CAC nor CALC demonstrated any discernible inhibitory effects on elevated body temperature in rats.

Subsequently, the changes in the AA metabolic pathway at 30 min were quantitatively analyzed using oxidative lipidomics by ultra performance liquid chromatography-Q-TOF/mass spectrometry (UPLC-Q-TOF/MS) in rat brain tissue to validate the biological processes following CA administration. The results demonstrated that the expression levels of various oxidized lipids, including AA, PGG2, PGH2, PGE2, and PGD2, were significantly elevated in the Mod group following LPS stimulation. However, there was no significant change observed in the expression of PGF2α and 12-HETE. CA treatment reversed the upregulation of AA, PGG2, PGH2, and PGE2 in rat brain tissue by modulating the AA-PGE2 pathway (Fig. 7B), but did not exert a significant effect on the expression of oxidized lipids involved in other metabolic pathways. The scheme in Fig. 7C illustrated that α,β-unsaturated aldehyde group targets mPGES1 to regulate the AA-PGE2 pathway to exert its antipyretic effects.

As a complex physiological phenomenon, fever is a biological response to external stimuli or internal factors. It occurs due to disturbances in thermal regulation caused by pyrogenic cytokines and pyrogens in response to inflammation and infection. The induction and sustenance of fever during infection involve a harmonized interaction between immune cells and neural circuitry systems [18]. Nonsteroidal anti-inflammatory drugs (NSAIDs) have been extensively utilized for the management of inflammatory diseases by suppressing upstream COX2 to reduce PGE2 levels [19]. However, high-dose administration targeting COX2/TXA2 inhibition may lead to gastrointestinal bleeding [20]. In the AA metabolic pathway, phospholipase A2 (PLA2) metabolizes phospholipids in the cell membrane to produce AA. COX1/2 catalysis converts AA into intermediate PGG2, which is then immediately transformed into PGH2 *via* peroxidase [21]. Finally, prostaglandin E synthases (PGESs) play a decisive role in the synthesis of PGE2 [13]. Arguably, directly targeting downstream mPGES1 instead of upstream COX1/2 may be preferable for selectively blocking overexpressed PGE2, without affecting other substrates generation such as PGD2, PGF2α or TXA2 in inflammatory diseases, which catalyzed by PTGDS, PGFS or TBXAS1. For example, the oral mPGES1 inhibitor ISC 27864 effectively suppressed the dose-dependent generation of inducible PGE2 (10–1000 mg) in comparison to celecoxib, as observed in a Phase I clinical trial study [22].

Previous studies revealed that CA possesses the ability to alleviate acute pain and inflammation, as well as improve arthritis in mice by inhibiting nitric oxide (NO), tumor necrosis factor-α (TNF-α), and PGE2 production [23–25]. Moreover, existing evidence supported that DAL impairs vascular endothelial function by negatively affecting mitochondrial function and autophagic flux [26,27]. Herein, we have discovered that certain antipyretic compounds including CA and DAL present in traditional heat-clearing herbs exert antipyretic effects *via* the irreversible targeting of mPGES1 on cerebral vascular endothelium. The isomerization of PGH2, catalyzed by mPGES1 to generate PGE2, requires the presence of glutathione as a cofactor in the TM4 helix active pocket [28]. We propose that the binding of α,β-unsaturated aldehyde compounds to the mPGES1-TM4 helix hinders the isomerization process, ultimately inhibiting PGE2 synthesis [10].

In summary, this study elucidated the mechanism by which CA and DAL covalently bind to mPGES1 in the cerebral vasculature, where they exert antipyretic effects by inhibiting the AA-PGE2 pathway and downregulating PGE2 expression in brain tissues. Targeting mPGES1-TM4 *via* α,β-unsaturated aldehyde represents a novel antipyretic mechanism, offering a fresh perspective for the development of mPGES1 inhibitors.

Declaration of competing interest

The authors declare that they have no known competing financial interests or personal relationships that could have appeared to influence the work reported in this paper.

CRediT authorship contribution statement

Fuyun Chi: Writing – original draft, Validation, Methodology, Formal analysis, Data curation. **Man Zhang:** Methodology. **Yiman Han:** Methodology. **Fukui Shen:** Methodology. **Shijie Peng:**

Methodology, Data curation. **Bo Su:** Methodology, Conceptualization. **Yuanyuan Hou:** Funding acquisition. **Gang Bai:** Writing – review & editing, Conceptualization.

Acknowledgment

This study was supported by the National Key R&D Program of China (Nos. 2022YFC3500800 and 2022YFC3500805).

Supplementary materials

Supplementary material associated with this article can be found, in the online version, at doi:10.1016/j.cclet.2024.109913.

References

[1] J. Singh, R.C. Petter, T.A. Baillie, et al., Nat. Rev. Drug Discov. 10 (2011) 307–317.
[2] F. Sutanto, M. Konstantinidou, A. Domling, RSC Med. Chem. 11 (2020) 876–884.
[3] M. Gersch, J. Kreuzer, S.A. Sieber, Nat. Prod. Rep. 29 (2012) 659–682.
[4] W. Xu, L. Ngo, G. Perez, et al., Proc. Natl. Acad. Sci. U. S. A. 103 (2006) 15540–15545.
[5] P. Hadvary, W. Sidler, W. Meister, et al., J. Biol. Chem. 266 (1991) 2021–2027.
[6] K. Uchida, Redox Biol. 1 (2013) 94–96.
[7] J. Yoshitake, T. Shibata, C. Shimayama, et al., Redox Biol. 23 (2019) 101115.
[8] C.T. Robb, M. Goepp, A.G. Rossi, et al., Br. J. Pharmacol. 177 (2020) 4899–4920.
[9] J.Y. Park, M.H. Pillinger, S.B. Abramson, Clin. Immunol. 119 (2006) 229–240.
[10] C. Jegerschöld, S.C. Pawelzik, P. Purhonen, et al., Proc. Natl. Acad. Sci. U. S. A. 105 (2008) 11110–11115.
[11] R.W. Friesen, J.A. Mancini, J. Med. Chem. 51 (2008) 4059–4067.
[12] D.K. Nomura, B.E. Morrison, J.L. Blankman, et al., Science 334 (2011) 809–813.
[13] T. Tanioka, Y. Nakatani, N. Semmyo, et al., J. Biol. Chem. 275 (2000) 32775–32782.
[14] K. Watanabe, K. Kurihara, Y. Tokunaga, et al., Biochem. Biophys. Res. Commun. 235 (1997) 148–152.
[15] X. Ma, Y. Han, K. Liu, et al., Chin. Chem. Lett. 34 (2023) 107595.
[16] P. Gao, J. Chen, P. Sun, et al., Chin. Chem. Lett. 34 (2023) 108296.
[17] D.B. Wilhelms, M. Kirilov, E. Mirrasekhian, et al., J. Neurosci. 34 (2014) 11684–11690.
[18] Z. Obermeyer, J.K. Samra, S. Mullainathan, BMJ 359 (2017) j5468.
[19] C. Walker, L.M. Biasucci, Postgrad. Med. 130 (2018) 55–71.
[20] C. Patrono, L.A. García Rodríguez, R. Landolfi, et al., N. Engl. J. Med. 353 (2005) 2373–2383.
[21] S. Das, S. Chandrasekhar, J.S. Yadav, et al., Chem. Rev. 107 (2007) 3286–3337.
[22] S. Sant, M. Tandon, V. Menon, et al., Osteoarthr. Cartilage 26 (2018) S351–S352.
[23] J. Liao, J. Deng, C. Chiu, et al., Evid. Base. Complement. Alternat. Med. 2012 (2012) 429320.
[24] L. Sun, S.B. Zong, J.C. Li, et al., J. Ethnopharmacol. 194 (2016) 904–912.
[25] S.H. Tseng, C.J. Lee, S.H. Chen, et al., J. Tradit. Complement. Med. 13 (2022) 51–61.
[26] Y. Hu, F. Yin, Z. Yu, et al., Redox Biol. 34 (2020) 101577.
[27] Y. Hu, G. Zhao, L. Qin, et al., Food Funct. 12 (2021) 5488–5500.
[28] A. Bresell, R. Weinander, G. Lundqvist, et al., FEBS J. 272 (2005) 1688–1703.